

Experimental Investigations on Magnetically Impelled Arc Butt Welded T91 Steel Tubes

S. Vignesh¹ · P. Dinesh Babu² · V. Prasanna Venkatesh² · S. Martin Vinoth² · P. Marimuthu²

Received: 27 November 2016 / Accepted: 13 February 2017 / Published online: 1 March 2017
© The Indian Institute of Metals - IIM 2017

Abstract Magnetically impelled arc butt welding (MIAB) is said to be a hybrid solid-state welding technique which is mainly preferred for butt welding of hollow cylindrical parts such as pipes and tubes. The MIAB setup is robust and fairly simple in design, and requires low upset pressure than the methods like Friction welding. This study investigates the effect of MIAB welding parameters on T91 steel tubes and the experimental observations on the welded joints. The input parameters considered in the present work are welding current (900, 1000, 1100 A), tube thickness (3.5, 4.5, 5.5 mm) and weld time (6, 9, 12 s). The tensile strength and hardness measurements have been recorded and the cross sectional micro and macro images have been observed for the welded samples. Further, the welded specimens have undergone computed tomography and radiography tests. It is concluded from the study that MIAB is one of the feasible welding techniques for joining steel tubes. However, the result shows crack in the weld zone for selected parameters. This defect may be avoided by selecting the optimum welding parameters.

Keywords MIAB welding · T91 steel tubes · Hardness · Micro-structure · NDT · Computed tomography · Radiography

1 Introduction

Magnetically impelled arc butt welding (MIAB) is said to be a reliable and superior welding method as it is a substitute to the conventional welding methods. The MIAB welding is a solid state welding technique which is used in steel pipes, tubes, etc. In this technique, the heat is generated prior to forging with the help of an electric arc moving along the peripheral edges of the weldments with the support from external magnetic field. The electromagnetic force is generated from the contact of the magnetic field between the gap and the arc current. This type of welding is achieved with the help of localized melting at the edges of the tubes and adjacent softening which is said to take place in the heat affected zone (HAZ). Further, the weld is obtained once the tubes are forged together. The schematic representation of MIAB welding process is shown in the Fig. 1. This welding process relies on the electric arc which in turn will generate the necessary heat to melt the faying surfaces. The electric arc generated helps in lowering the yield strength of nearby material to get prepared with enough forging action which is mostly required for producing the joints.

As shown in Fig. 1, the electric arc will spin around the weld specimens due to the presence of the magnetic field. The velocity of the arc can be about 200 m/s and when combined with the thermal conductivity of the metal being welded, it tends to produce uniform heating at the joint. At the end of the heating phase, the tubes are brought closer under pressure. This step squeezes the molten material out of the joint and tends to create a forging action on the remaining plasticized metal. Finally, the solid-state joint can be achieved. This process does not use filler metal. The need of shielding gas is usually not required, though rarely used. A short pulse of high current is added so as to expel

✉ P. Dinesh Babu
pdineshbabu81@gmail.com

¹ Department of Mechatronics, Bannari Amman Institute of Technology, Sathyamangalam, India

² School of Mechanical Engineering, SASTRA University, Thanjavur, India

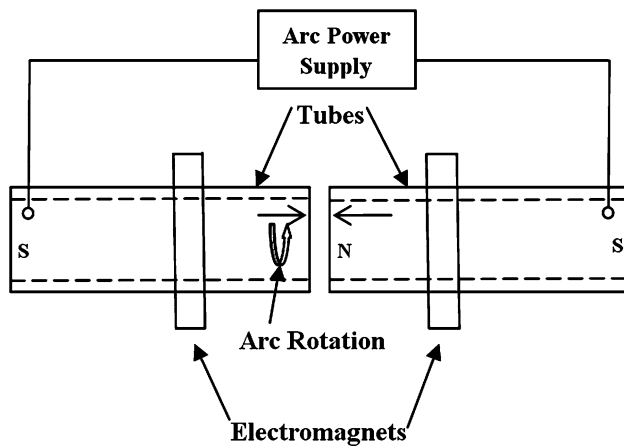


Fig. 1 Line diagram of MIAB welding technique

the contaminated molten metal prior to upset, when the shielding gas is not used.

Taneko et al. [1] investigated the arc angles and arc velocities using a voltage detector kept at various locations inside an alloy steel tube, a high speed video camera and an oscilloscope. They examined the relationship between the position at which power was supplied to the tubes, arc angle and the arc velocity, and decided that the arc blow effect and low electrical resistance of the tube caused the increase in current in the arc. A new perspective was presented by Fletcher et al. [2]. They designed a model of the MIAB welding equipment. The prototype was much capable to weld natural gas pipelines. In the research work carried out by Xiancong et al. [3], they shared the investigation reports on the subject of heat flow in the MIAB weld joint. They assumed the rotating arc to be a constant heat source and framed a heat flow equation for determining the value of temperature at time 't' and distance 'y' from the arc. The evaluation of the effect of arc gap variations and weld parameters was performed by Yatsenko et al. [4] after studying the velocity of the arc movement in the gap between a plate and tube. Arungalai Vendan et al. [5] attempted to build up a MIAB welding machine for better understanding on the importance of different process variables.

Iordachescu et al. [6] examined the relations between the arc and magnetic field in MIAB welding of steel tubes. They developed operational process windows for attaining good MIAB joints. Arungalai Vendan et al. [7, 8] attempted to build up a MIAB welding unit operated pneumatically for the process. They conducted tests with alloy steel tubes by changing the input variables. They identified the suitable ranges of input process parameters based on the depth and weld bead. Also, they carried out non-destructive tests on the MIAB welded samples. They

concluded that MIAB had several advantages in terms of its metallurgical integrity, quality and strength. Arungalai Vendan et al. [9] studied the feasibility of MIAB welding process for joining alloy tubes. The strength of MIAB welded specimens were examined by subjecting the welded specimens to various destructive tests and observed that the weld region was stronger than the base metal in most of the cases. Sivasankari et al. [10] studied the microstructural changes occurring in thermo-mechanically affected zone formed in MIAB welding of T11 steel tubes. They found that the weld zone showed higher hardness than that of base metal and indicated higher weld tensile strength and ductility due to bainitic transformation.

Though, several studies [1–10] have been done on MIAB welding, there are no reports showing the observations on welding T91 steel tubes. Further, the computed tomography (CT) and radiography tests (RT) have not been reported much in the literatures. There are very few literatures available related to the investigation on MIAB welded steel tubes with NDT 3D analysis. Hence, an attempt has been performed to weld T91 steel tubes. Thus, the present work investigates the parameters involved in producing MIAB welded joints of T91 tubes. The steel tubes have been chosen as it is widely used in boiler applications. For all the experimental trials, T91 tubes have been used as it has high percentage of chromium content and gives higher thermal conductivity to the material. The chemical composition and mechanical properties of T91 steel tubes are shown in Tables 1 and 2 respectively. The effect of other elements like Molybdenum, Carbon, and Manganese will increase the strength of the material. The selected material should have high thermal conductivity in the process of MIAB welding.

2 Experimental Setup and Process Parameters

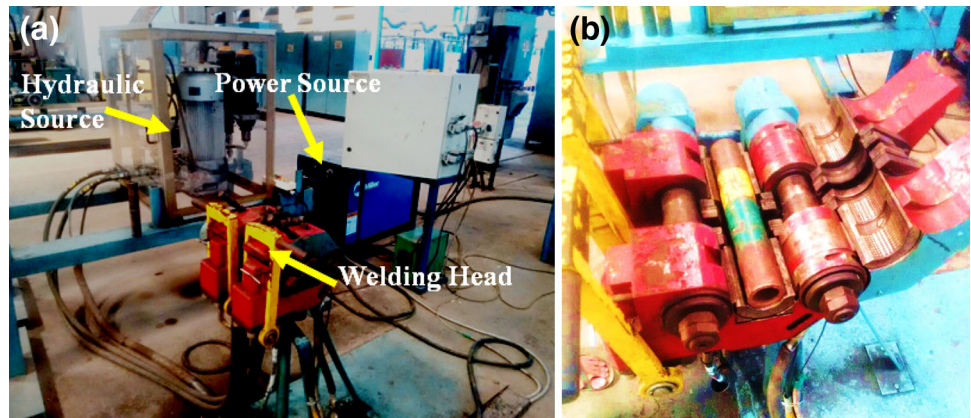
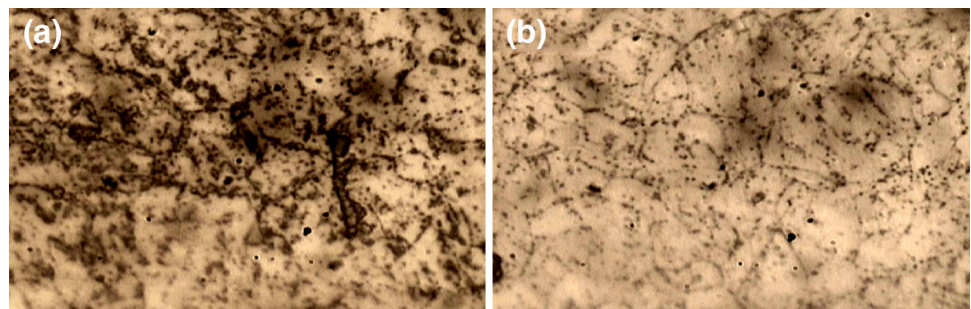
The MIAB welding unit shown in Fig. 2 had three main components as hydraulic source, welding head, and power source. In this setup, one tube was considered to be rigid and the other tube was changeable. The linearly movable tube was joined to a motor. The distance between the tubes could be adjusted from 10 to 15 mm using the movable jaw. The magnetic coil arrangement in the welding unit comprised of a covered core with coils. When the coil was motorized, an arc struck between the tubes and started to rotate at a lower speed of about 75 rpm. Sufficient number of trials were conducted with the help of ESAB power source which was available at welding research institute (WRI), Bharat Heavy Electricals Limited (BHEL), Tiruchirappalli. The hydraulic clamping was used to clamp

Table 1 Chemical composition of T91 steel tubes in weight percentage

C (%)	Si (%)	Mn (%)	Cr (%)	Mo (%)	Ti (%)	Nb (%)	P (%)	S (%)	Balance
0.15	0.24	0.43	8.84	0.99	0.19	0.10	0.02	0.01	Fe

Table 2 Mechanical properties of T91 steel tubes

Yield strength (MPa)	Tensile strength (MPa)	Elongation (%)	Hardness (HRB)
415	585	20	25

Fig. 2 MIAB welding equipment; **a** arrangement showing the various units; and **b** closer view of the setup (WRI—BHEL, Trichy)**Fig. 3** Microstructure of base metal T91 Specimen; **a** at $\times 500$ magnification; and **b** at $\times 250$ magnification

the two tubes. The modification was done in the magnetic coil unit to achieve an enhanced arc rotation. The solid core design was chosen instead of laminated core due to the issue faced in magnetic saturation. The tube of diameter 44.5 mm was split into two pieces and located at the ends of the solid core. It was identified that the arc rotation behaviour mainly depended on three parameters such as coil position, gap size and exciting current.

The microstructure of the base metal (T91 steel tube) was examined for different magnifications and is reported in Fig. 3. The parameters necessary for MIAB welding process was identified and listed in Table 3. The parameter levels were chosen with three intervals. The chosen parameters and ranges could help us to get desired rate of heating effect which would raise the temperature of the

tube to be welded. The constant factors involved in the welding process are listed in Table 4. With the help of Design Expert software, the design matrix was generated considering the factors and levels required. The design of experiments (DOE) was an approach to determine the number of trials to be performed. The parameter window is shown in Table 5.

2.1 Preparation of Material

The tubes to be welded were cut into two halves using power hacksaws. The cutting process was followed by boring operation using four jaw chuck lathe. The second step was carried out mainly to increase the internal diameter of the tubes thereby reducing the thickness of

Table 3 Parameter levels in the welding process

Parameter	Unit	Level 1	Level 2	Level 3
Upsetting current	Ampere	900	1000	1100
Welding time	Seconds	6	9	12
Tube thickness	Millimetres	3.5	4.5	5.5

Table 4 Constant factors involved in the process

Sl. no.	Description	Measured value
1	Diameter of the tube	44.5 mm
2	Length of the tube	250 mm
3	Cross sectional area	741 mm ²
4	Upsetting pressure	150 N/mm ²

Table 5 Parameter window for welding T91 tubes

Sl. no.	Upsetting current (A)	Welding time (s)	Tube thickness (mm)
1	900	6	3.5
2	900	9	4.5
3	900	12	5.5
4	1000	6	3.5
5	1000	9	4.5
6	1000	12	5.5
7	1000	6	4.5
8	1100	6	3.5
9	1100	9	4.5
10	1100	12	5.5

it. Finally, the facing operation was done so that charges could flow easily through the tube edge surfaces. The size of T91 tubes before welding was found to be of length 500 mm, outer diameter 44.5 mm and thickness 5.7 mm.

2.2 Initial Setting in the Welding Unit

The run orders determined using DOE had to be fed in the welding unit as an initial setting. The default factors such as voltage, current, temperature and the corresponding run orders had to be fed. The tube to be welded was placed and locked between the two jaws of the setup.

2.3 MIAB Welding of T91 Steel Tubes

Once the initial setting was done, the T91 steel tubes were welded for ten different run orders and the welded tubes are shown in Fig. 4. The tubes were placed at the centre of the setup so that the magnetic field acted exactly at the centre of the tubes. The alignments of tubes were checked and the welding process started by arc initiation with the current I_1 .

The current required for arc initiation was high. The step 2 dealt with the arc stabilization and arc rotation, and it required fewer amounts of current I_2 and I_3 . Finally, the current required for upsetting was allowed to pass through the tubes so that the welded tubes could be removed easily from the clamp. Similarly, the above steps were repeated for 10 different run orders.

3 Result and Discussions

After the joining of T91 steel tubes using MIAB welding process, several investigations have been carried out to ensure the stability of the welded joints.

3.1 Measurement of Temperature in the Heat Affected Zone (HAZ)

The temperature measurement in heat affected zone of MIAB welded joints has been done with the help of Temperature Time Indicator (TTI). TTI is a device that shows the accumulated time temperature history of the welded joint. The temperature measurement is done in the heat affected zone (HAZ) in all the welded tubes. The measured temperature details (°C) in the HAZ have been listed for each run order in Table 6. The thermocouple is used as a sensor in temperature data logger. The two ends of the thermocouple are connected to the back side of the logger through which the readings are recorded in the logger. The type of thermocouple used in this measurement is K-type.

When the upsetting current is higher (1100 A) for the tube thickness of 5.5 mm, the welding time is found to be 12 s. The measured temperature (992 °C) in the heat affected zone at this parameter level is considered maximum. This clearly indicates that the heat accumulation is less in the welded tubes, and the very narrow zone will get affected by the heat during welding. It is also observed during the study that the welded tubes can be handled without any safety gloves or other holding devices, which confirms the fast cooling rate of the MIAB welding process. The obtained low temperature (<1000 °C) in the HAZ predicts that the possibility for distortion is less in the welded region.

Fig. 4 T91 tubes after MIAB welding

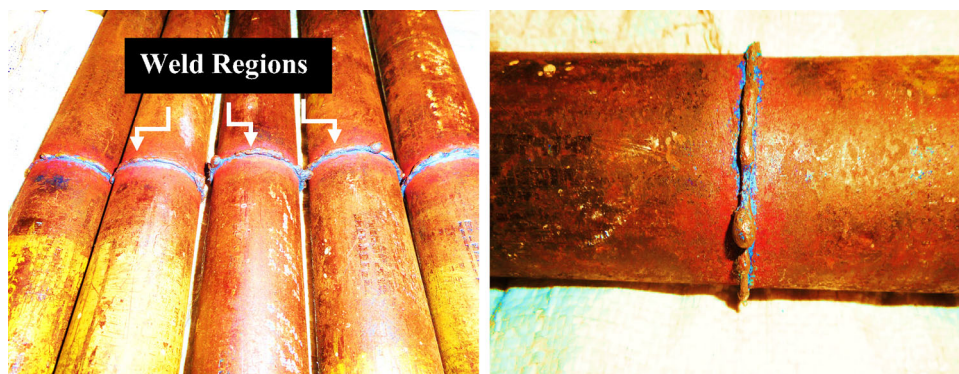


Table 6 Temperature at the heat affected zone for different parameter levels

Sl. no.	Upsetting current (A)	Welding time (s)	Tube thickness (mm)	Temperature at HAZ (°C)
1	900	6	3.5	952
2	900	9	4.5	964
3	900	12	5.5	987
4	1000	6	3.5	960
5	1000	9	4.5	966
6	1000	12	5.5	989
7	1000	6	4.5	963
8	1100	6	3.5	950
9	1100	9	4.5	972
10	1100	12	5.5	992

3.2 Measurement of Tensile Strength

The MIAB welded T91 steel tubes have been subjected to tensile testing. The ASTM 8 standard has been chosen for conducting the test. Three welded specimens (900, 1000, 1100 A current with constant tube thickness and welding time) have been chosen for the tensile test. Figure 5 shows the welded specimens after subjected to tensile test. The Table 7 shows the result obtained after tensile test.

Fig. 5 Welded specimens after tensile test



The result obtained from tensile test confirms the fracture occurred in the weld region for the selected samples due to the crack formation in the weld area. Table 7 shows that when upsetting current is more (1100 A) the tensile strength will be low; this is due to high hardness obtained by high current. On the whole, tensile strength of the MIAB welded specimens are low compared with base metal strength (550 N/mm²).

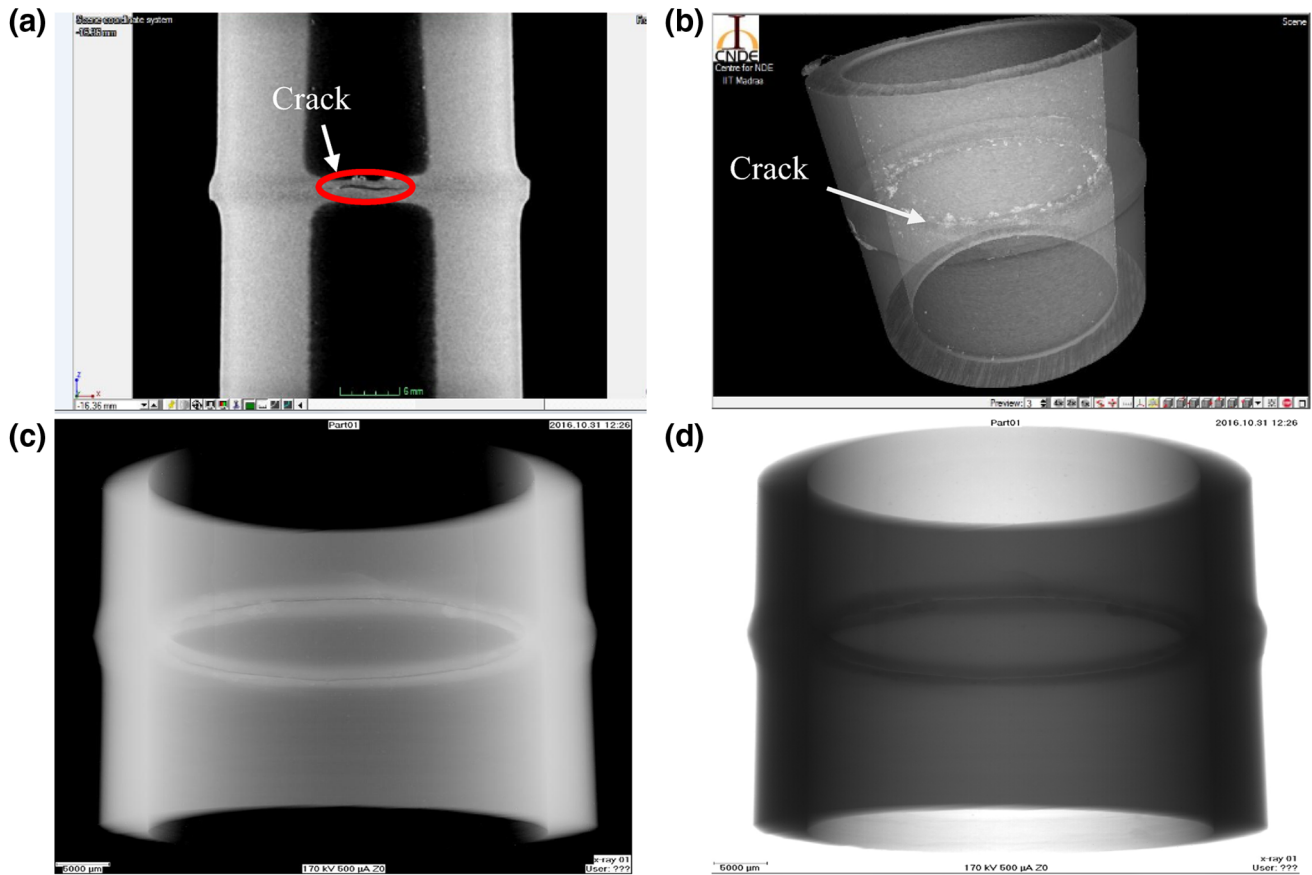
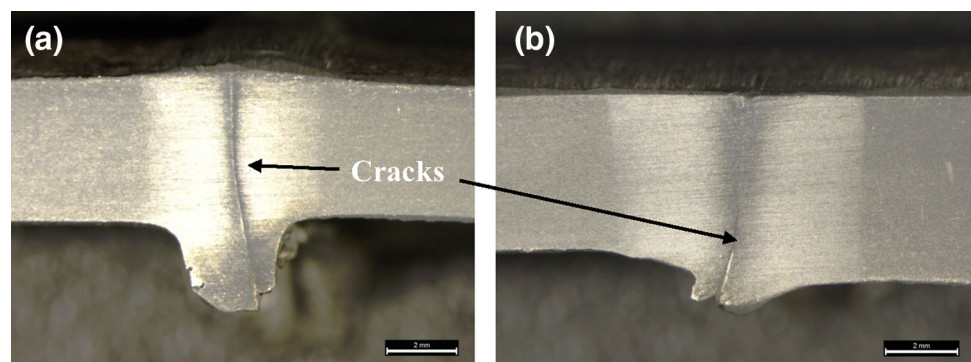
3.3 Non Destructive Testing

Non-destructive testing (NDT) helps in finding the weld defects in order to avoid the major failure to occur in the welded parts. Computed tomography (CT) is a non-destructive testing technique newly recognized particularly in the detection of defects. The performance of 3D images by micro-focus computed tomography begins with 2D images of the test part projections developed by gradual revolving of the test piece within the limit of X-ray direction. The sample rotation is executed slowly at <math><1^\circ</math> provided the specimen is radiated from all regions.

The computed tomography (CT) and radiography test (RT) results of the weld tubes are shown in Fig. 6. The results of CT and RT examinations show 3D images of the welded tubes. No defect is identified on the surface of the weld through visual inspection. When examined through CT and RT, it is observed that the samples have several

Table 7 Tensile test results of welded samples

Sl. no.	Upsetting current (A)	Welding time (s)	Tube thickness (mm)	Tensile strength (N/mm ²)	Point of fracture
1	900	12	5.5	350	Weld metal
2	1000	12	5.5	310	Weld metal
3	1100	12	5.5	280	Weld metal

**Fig. 6** Radiography images of welded tubes at welding current 900 A, 4.5 mm thickness; **a** CT—front view, **b** CT—3D view and **c**, **d** RT—3D view (negative)**Fig. 7** Macro section of MIAB welded specimens; **a** welding current 900 A, thickness 4.5 mm and **b** welding current 900 A, thickness 5.5 mm

defects and incomplete fusion areas. The NDT results confirm that cracks are formed in the weld region for the parameter level of welding current 900 A and tube thickness 4.5 mm.

From the overall observation from this study, it has been planned to do the parameter optimization for different upsetting currents based on the tube thickness, welding time and initial setup gap for the T91 steel tubes

in the future research to eliminate crack and incomplete fusion.

3.4 Macro Analysis

As indicated in Fig. 7, the cracks are observed in the fusion zone in 4.5 mm and 5.5 mm thick tubes for 900 A current. In the samples welded with lower arc rotation (900 A), the crack is said to occur at the weld interface due to the presence of metallurgically weak structures like voids at

weld interface. The higher amount of chromium content available in the steel tube may also contribute to the formation of cracks in the weld interface.

3.5 Analysis of Micro Hardness

The hardness measurement helps in ensuring the performance of the boiler tubes with particular physical properties. The hardness test has been conducted using Vickers hardness tester with 10 N load for 15 s duration. The measurement of hardness has been carried out at three different welding parameter levels. The micro hardness of the MIAB welded tubes are shown in Fig. 8. The variation of hardness is examined at three different zones such as weld zone, heat affected zone and in the base metal. This study has been carried out for different rotating arc current (900, 1000, 1100 A) subjected to constant specimen thickness of 5.5 mm. The hardness measured in the weld region is superior to the heat affected zone in all the three cases and very narrow HAZ is obtained in the welded samples in the range of 1 mm.

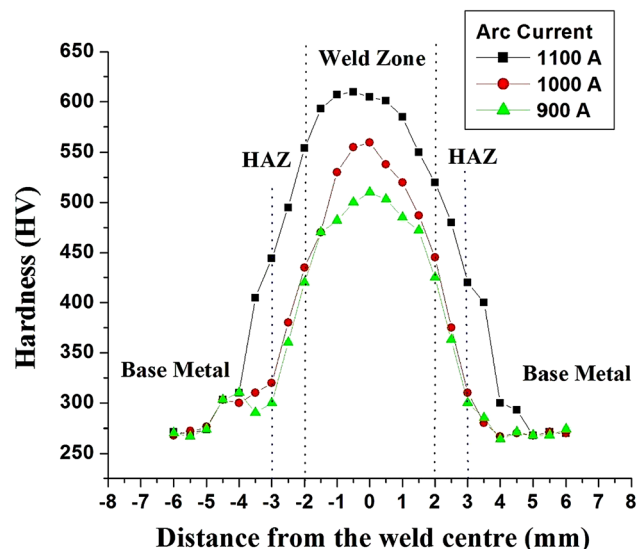
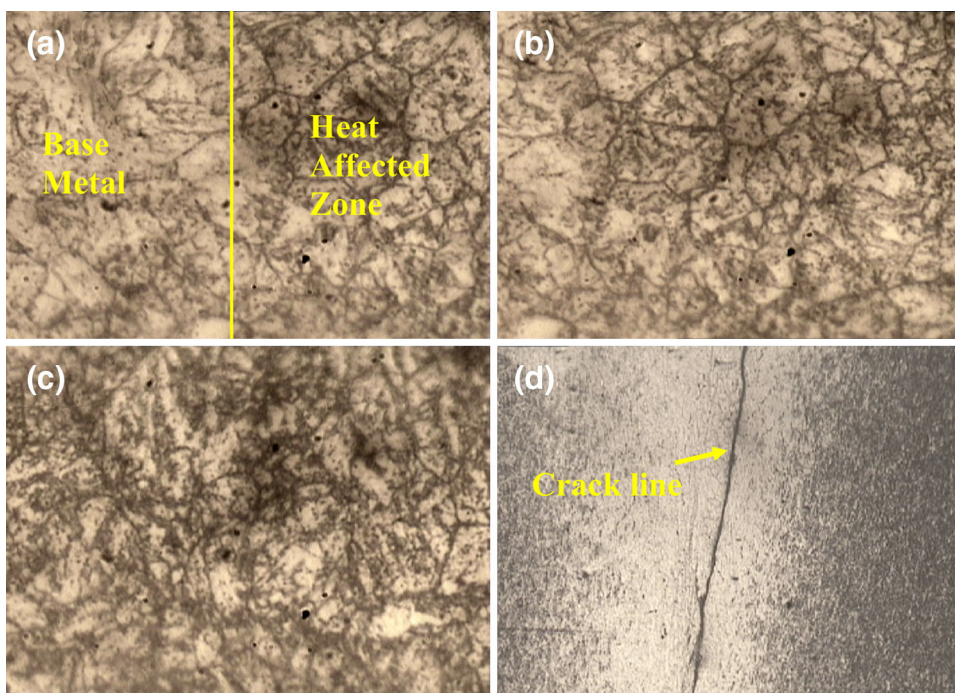


Fig. 8 Hardness variation in the weld area, HAZ and base metal for different rotating arc current for constant 5.5 mm thick specimens

The hardness trend observed in Fig. 8 confirms that when the arc current is said to be high (1100 A), an enormous amount of heat is generated by the magnetic field induced between the tubes. It results in rapid cooling in the weld zone and leads to higher hardness of around 600 HV. On the other hand, when the arc current is low (900 A), the heat induced is less in the joining region of tubes. This tends to result in lower hardness of about 500 HV.

Fig. 9 Microstructure of the welded sample; a transition zone at $\times 1000$, b HAZ at $\times 1000$, c weld zone at $\times 1000$ and d weld zone



3.6 Micro Analysis

The microstructure of the base metal (Fig. 3) confirms ferrite and pearlite structure. In the thermo mechanically affected zone of the welded sample as shown in Fig. 9, it is observed that bainite structure is formed in the weld region along with polygonal ferrite. Deformation occurs during the upsetting of tubes holds up the development of bainitic structure. Figure 9a shows the transition zone of base metal and heat affected zone clearly. Figure 9b shows the coarse grain structure formed in the HAZ due to low thermal effect caused during this welding process. A narrow HAZ is formed due to higher heat input and very low weld cycle, i.e., 12 s for the sample. Figure 9c confirms the fine grain structure formed in the fusion zone due to high arc rotation. During arc rotation, an overheated area is created in spots on the welding arc. During the upset time, the coarse-grain area is pushed out into pre-external support and spark, and the joint is produced at the cost of the fine-grain area. This micro-graph (Fig. 9d) also confirms the crack formation due to high chromium content present in the metal.

4 Conclusions

The study on MIAB welding of T91 steel tubes was carried out. The following observations were made based on this investigation.

1. The feasibility of MIAB welding of T91 steel tubes was established and authentically verified.
2. The possibility of MIAB weld interface failures as a result of the presence of chromium enriched areas at the weld interface was identified. The chromium enriched regions were mostly oxides that were produced during arcing progression and in the later stage it requires more attention in the joint.
3. Computer tomography stood to be a consistent and precise NDT method for analysis of interior defects in welded samples. MIAB weld quality was analysed with RT and CT images and it confirmed the crack formation in the weld region for the selected parameters, which in turn led to poor tensile strength.
4. The hardness in the weld zone increased with the arc current increment.
5. The future research on T91 steel tube joints should focus specifically on the wide range of initial setup gaps to determine whether or not gap length played an important role in the presence of chromium at the weld interface.

Acknowledgements The authors are grateful to Welding Research Institute at BHEL Trichy, Centre for Non-destructive Evaluation at Indian Institute of Technology Madras and School of Mechanical Engineering SASTRA University for providing facilities to carry out this investigation.

References

1. Taneko A, Arakida F, and Takagi K, *Weld Int* **3** (1987) 247.
2. Fletcher L, Stecher G, and Stubbs G, in *Proceedings of the International Conference on Pipeline Construction Technology* (2005), p 1.
3. Xiancong, and Ruilin, in *Proceedings of the Welding Institution of the Chinese Mechanical Engineering Society* (1984), p 1.
4. Yatsenko K, Syrovatka, and Kuznetsov, *Autom Weld* (1983) 23.
5. Arungalai Vendan S, Manoharan S, Buvanashakaran G, and Nagamani C, *Int J Multidiscip Model Mater Struct* **5** (2009) 229.
6. Iordachescu D, Iordachescu M, Georgescu B, Miranda R M, Ruiz-Hervias J, and Ocana J L, *J Mater Process Technol* **210** (2010) 951.
7. Arungalai Vendan S, Manoharan S, Buvanashakaran G, and Nagamani C, *Mechat* **21** (2011) 30.
8. Arungalai Vendan S, Manoharan S, and Nagamani C, *J Manuf Process* **14** (2012) 82.
9. Arungalai Vendan S, Manoharan S, Buvanashakaran G, and Nagamani C, *J Manuf Process* **14** (2012) 328.
10. Sivasankari R, Balusamy V, Venkateswaran P R, Buvanashakaran G, and Ganesh Kumar K, *Def Technol* **11** (2015) 244.